AAS 01-380

MOMENTUM MANAGEMENT FOR THE MESSENGER MISSION

Robin M. Vaughan[†], David R. Haley[†], Hongxing S. Shapiro[†], and Daniel J. O'Shaughnessy[†]

The MESSENGER – MErcury Surface, Space ENvironment, GEochemsitry, and Ranging - spacecraft will be the first spacecraft to closely observe the planet Mercury since the Mariner 10 flybys of the mid-1970s. Scheduled for launch in 2004, MESSENGER will orbit the planet for one Earth-year beginning in April of 2009. Reaction wheels will be the primary actuators for attitude control, making momentum management an essential guidance and control task. This paper summarizes momentum modeling for the MESSENGER spacecraft and discusses momentum management strategies that will be used during the mission. The main external torques contributing to momentum accumulation are due to solar pressure acting on the spacecraft's sunshade and solar panels. Analytic models of these effects are derived and used to simulate momentum build-up during typical mission operations in orbit about Mercury. Results are presented to illustrate the trade-off between reaction wheel storage capacity, active offloading of momentum using thruster dumps, and passive reduction of system momentum using solar torque generated from solar pressure on the spacecraft's sunshade. Momentum targeting using solar torque is shown to be a valuable tool for momentum management, reducing the frequency at which thruster dumps will need to be performed.

INTRODUCTION AND MISSION OVERVIEW

MESSENGER is a scientific investigation of the planet Mercury. Understanding Mercury, and the forces that have shaped it, is fundamental to understanding the terrestrial planets and their evolution.[1] The spacecraft is scheduled for launch in 2004 and will perform two flybys of Venus followed by two flybys of Mercury prior to entering orbit about the planet in 2009. The orbital phase will use the data from the Mercury flybys as an initial guide to perform a focused scientific investigation of the planet. MESSENGER will gather data to answer key scientific questions regarding Mercury's characteristics and environment during these two complementary mission phases. Science observations are performed by an optimized set of miniaturized space instruments and the spacecraft telecommunications system.[2] MESSENGER will enter Mercury orbit in April 2009 and carry out comprehensive measurements for one Earth year. Orbital data collection concludes in April 2010.

The spacecraft design[3] is driven by the thermal and radiation environment at Mercury. A large sunshade is used to protect most of the spacecraft systems from the heat and radiation of the Sun as shown in Figure 1. The primary structure is made of composite walls forming three compartments housing the main fuel and oxidizer tanks. Two solar panels are used to power the

[†] Space Department, Mission Concept and Analysis Group, The Johns Hopkins University Applied Physics Laboratory, Laurel, Maryland.

spacecraft. The panels have power-generating cells on one side and can be rotated about a single axis to track the Sun direction. The spacecraft carries two sets of high- and medium-gain antennas for communication with Earth, mounted on opposite sides of the spacecraft. The spacecraft also carries four low-gain antennas. The orbit insertion engine is mounted on the top of the structure as indicated in the figure. Most of the science instruments are mounted inside the launch vehicle adapter that attaches to the bottom of the structure on the opposite side from the orbit insertion engine.

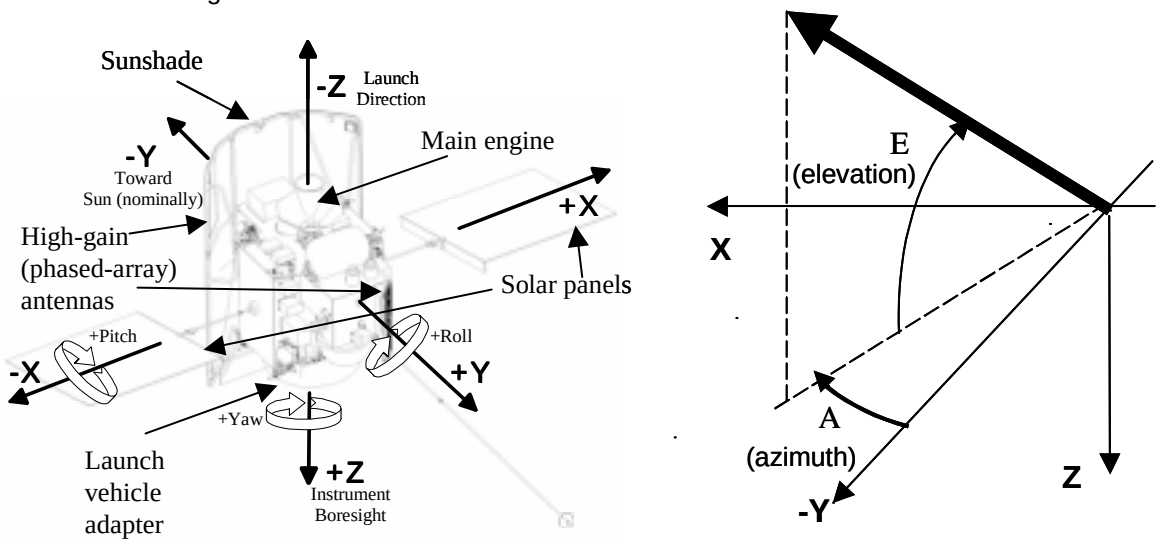

Figure 1 MESSENGER Spacecraft and Body Coordinate System

The MESSENGER guidance and control system maintains a 3-axis stabilized spacecraft using reaction wheels as the primary actuators for attitude control. Star trackers and an inertial measurement unit containing four gyros provide knowledge of inertial attitude and rotation rates. Sun sensors are used to provide Sun-relative attitude knowledge as a backup to the inertial sensors for spacecraft safety. The propulsion system has a large bi-propellant engine and two sets of mono-propellant thrusters. The main engine will be used for orbit insertion and other large velocity change maneuvers. Some combination of the ten 4-N and the four 22-N mono-propellant thrusters will be used to offload momentum from the reaction wheels and as a backup system for attitude control.

The use of reaction wheels for attitude control makes momentum management an important responsibility of the MESSENGER guidance and control subsystem. This paper describes the key issues associated with momentum management during the orbital phase of the mission. The first section gives background material such as spacecraft coordinate system definitions used throughout the remainder of the paper. Then, analytic models for the torques due to solar pressure acting on the spacecraft's sunshade and solar panels are presented. Next, the sunshade solar torque model is used to derive formulas for determining a spacecraft attitude that can achieve a desired momentum target while simultaneously satisfying mission constraints on Sun exposure and maintaining phased-array antenna communications with Earth. The final sections describe the simulation developed to model on-orbit momentum accumulation and present results obtained using different momentum management strategies. The effectiveness of the different strategies are compared in terms of number and time separation of thruster dumps required over a typical 90-day period. The factors that most strongly influence the frequency of thruster dumps are shown to be the momentum storage capacity of the reaction wheels and the size of the offset between the spacecraft center of mass and the "center" of the sunshade relative to solar pressure.

SPACECRAFT COORDINATE SYSTEM

The body frame for the MESSENGER spacecraft is defined as shown in Figure 1. The origin is located at the geometric center of the oxidizer tank, which is the middle of the three main tanks of the propulsion system. The positive Z-axis points toward the launch vehicle adapter where the science instruments are housed, the negative Y-axis points out away from the sunshade, and the X-axis completes a right-handed coordinate system and is the nominal rotation axis for the solar panels. The terms pitch, yaw, and roll refer to rotations about the –X, +Z, and –Y axes, respectively.

Directions in the body frame can be expressed as unit vectors or by an azimuth and an elevation angle. Referring to Figure 1, the azimuth angle, denoted A, is the angle in the XY plane measured clockwise from the –Y axis to the projection of the unit vector in the XY plane. The elevation angle, denoted E, is the angle between the unit vector and the XY plane of the body frame. Elevation is considered to be positive for vectors on the –Z side of the XY plane and negative for vectors on the +Z side of the plane. Thus a unit vector $\hat{u}$ in the body frame can be expressed as $\hat{u} = \begin{bmatrix} u_x & u_y & u_z \end{bmatrix}^T = \begin{bmatrix} \cos\mathrm{E}\sin\mathrm{A} & -\cos\mathrm{E}\cos\mathrm{A} & -\sin\mathrm{E} \end{bmatrix}^T$ where $-\pi \le \mathrm{A} \le \pi$ and $-\pi/2 \le \mathrm{E} \le \pi/2$.

The sunshade is designed to provide adequate protection to spacecraft components over a limited range of Sun directions. Generally, the allowable locations for the Sun direction are restricted to azimuth and elevation angles within ranges symmetric about zero. These locations correspond to restrictions on pitch and yaw rotations of the spacecraft from the default attitude where the Sun direction is along the –Y body axis. There are no restrictions on roll; a rotation of any amount about the Y-axis is permitted. The space of attitudes that result in Sun directions within the allowable azimuth and elevation ranges is called the Sun keep-in zone. The unit vector pointing to the Sun must be kept in this zone at all times while in orbit about Mercury. Currently the keep-in zone limits are approximately $-13^\circ \le \mathrm{E} \le +13^\circ$ and $-15^\circ \le \mathrm{A} \le +15^\circ$.

SOLAR TORQUE AND MOMENTUM MODELS

The solar torque induced by sunlight hitting exposed parts of the spacecraft will be the primary external torque acting on the spacecraft. The dominant contributor to solar torque will clearly be the sunshade, but the two solar panels will also make a contribution. This section presents analytic expressions for the solar torque due to the sunshade and solar panels. The torque is shown to depend on the location of the shade or panel center relative to the spacecraft center of mass, their size and shape, and the reflectance properties of the surface materials exposed to the sunlight. Since the shade is fixed in the spacecraft body frame, the solar torque can be expressed as a polynomial in the components of the unit vector giving the direction to the Sun. A common formulation applies to both a simple cylindrical section and sets of intersecting polygonal faces for the sunshade. The solar panels will rotate in the spacecraft body frame to maintain the desired Sun-relative orientation for generating power. Solar torque for the panels is shown to be a function of both Sun direction and the orientation of the panel relative to the main body of the spacecraft.

Sunshade Solar Torque Models

The sunshade will be made from a ceramic cloth attached to a rigid frame constructed from titanium tubing. The initial design used curved tubing sections to produce a shade in the shape of a cylindrical section as shown in Figure 2(a). The design has since evolved to a frame having only linear segments for which the shade is more closely approximated by a series of contiguous rectangular plates shown in Figure 2(b). For generality, introduce a new coordinate system called the shade frame in which the sizes, shapes, and positions of the cylindrical section or rectangular plates are given; the orientation of this frame is fixed relative to the spacecraft body frame; ideally its axes are exactly aligned with the axes of the body frame. The solar radiation force acting on a surface element dA in the shade frame is

$$d\vec{F} = -P\{(1-C_s)\hat{s} + 2[C_s(\hat{n}\cdot\hat{s}) + \frac{1}{3}C_d]\hat{n}\}(\hat{n}\cdot\hat{s})dA$$
$$P = F_e / \left(c\, D_s^2\right) \tag{1}$$

where F_e is the solar flux constant at 1 AU, c is the speed of light, D_s is the distance of the spacecraft from the Sun given in AU, $\hat{n}$ is the unit, outward-pointing vector normal to the surface element, dA is the area of the element, $\hat{s} = \left[s_x \; s_y \; s_z\right]^{\mathrm{T}}$ is the unit vector pointing toward the Sun, and C_s and C_d are the specular and diffuse reflectivity coefficients of the shade material, respectively.[4] The total solar torque due to the sunshade is given by the integral of the differential torques over the entire surface

$$\vec{N} = \left[N_x \; N_y \; N_z\right]^{\mathrm{T}} = \int \vec{r} \times d\vec{F} \tag{2}$$

where $\vec{r}$ is the vector from the spacecraft center of mass to the surface element. Integrating this equation for both a cylindrical section or a series of plates gives the polynomial

$$\begin{aligned} N_j = P(&k_{j\_x}s_x + k_{j\_y}s_y + k_{j\_z}s_z + k_{j\_xy}s_x s_y + k_{j\_xz}s_x s_z + k_{j\_yz}s_y s_z \\ &+ k_{j\_xx}s_x^2 + k_{j\_yy}s_y^2 + k_{j\_zz}s_z^2) \end{aligned} \tag{3}$$

for the components of $\vec{N}$ where $j \in \{x, y, z\}$ and where the k coefficients depend on the shade shape as defined in the following paragraphs.

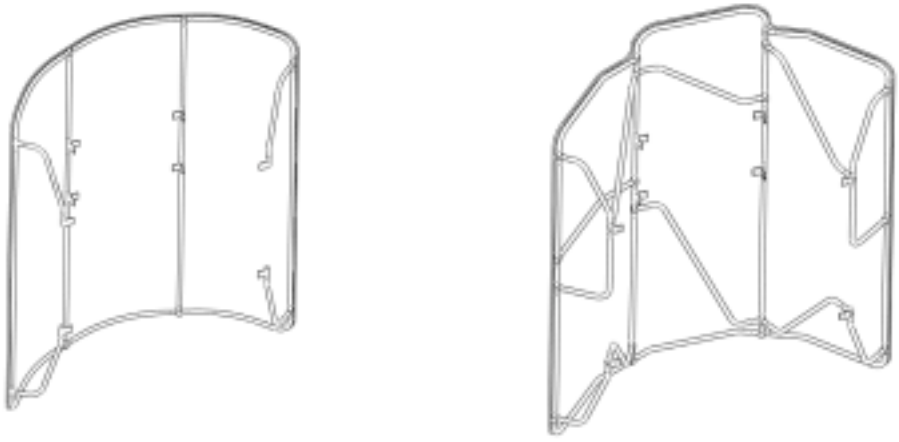

(a) Original cylindrical section **(b) Current faceted surface**

Figure 2 MESSENGER Sunshade Configurations

For the curved frame, the shade is modeled as a section of a cylinder of total height $2h_0$ along the Z-axis and radius R in the XY plane whose center is at the origin of the shade frame. The section subtends an angle of θ_0 along each side of the YZ plane on the –Y side of the XZ plane. Further assuming that C_s and C_d are constant over the cylindrical section, the non-zero coefficients in Eq. (3) for the solar torque are given by

$$
\begin{aligned}
k_{x\_y} &= -2Rh_0\{\frac{2}{3}z_c C_d \theta_p\} \\
k_{x\_yz} &= -2Rh_0\{(1-C_s) \\
&\quad [R\theta_p + 2y_c\theta_s]\} \\
k_{x\_xx} &= 2Rh_0\{\frac{4}{3}z_c C_s \theta_3\} \\
k_{x\_yy} &= 2Rh_0\{2z_c[(1+C_s)\theta_s - \\
&\quad \frac{2}{3}C_s\theta_3]\}
\end{aligned}
\qquad
\begin{aligned}
k_{y\_x} &= 2Rh_0\{\frac{2}{3}z_c C_d \theta_m\} \\
k_{y\_xy} &= -2Rh_0\{2z_c[(1-C_s)\theta_s + \\
&\quad \frac{4}{3}C_s\theta_3]\} \\
k_{y\_xz} &= 2Rh_0\{R(1-C_s)\theta_m\} \\
k_{y\_yz} &= 2Rh_0\{2x_c(1-C_s)\theta_s\}
\end{aligned}
\qquad
\begin{aligned}
k_{z\_x} &= -2Rh_0\{\frac{2}{3}y_c C_d \theta_m\} \\
k_{z\_y} &= 2Rh_0\{\frac{2}{3}x_c C_d \theta_p\} \\
k_{z\_xy} &= 2Rh_0\{R(1-C_s)\theta_2 + \\
&\quad 2y_c[(1-C_s)\theta_s + \\
&\quad \frac{4}{3}C_s\theta_3]\} \\
k_{z\_xx} &= -2Rh_0\{\frac{4}{3}x_c C_s \theta_3\} \\
k_{z\_yy} &= -2Rh_0\{2x_c[(1+C_s)\theta_s - \\
&\quad \frac{2}{3}C_s\theta_3]\}
\end{aligned}
\tag{4}
$$

where

$$
\theta_m = (\theta_0 - \frac{1}{2}\sin 2\theta_0) \quad \theta_p = (\theta_0 + \frac{1}{2}\sin 2\theta_0) \quad \theta_3 = \sin^3\theta_0 \quad \theta_s = \sin\theta_0 \quad \theta_2 = \sin 2\theta_0 \tag{5}
$$

and $\vec{r}_c = [x_c \;\; y_c \;\; z_c]^T$ is the vector from the origin to the spacecraft center of mass expressed in shade frame.[5] All of the other k coefficients are zero for the cylindrical section.

For the frame with linear segments, solar torque is generated from each face or plate in the shade. Assuming that the reflectivity coefficients are uniform over the entire plate surface, the coefficients in the polynomial for $\vec{N}$ due to a single plate are given by

$$
\begin{aligned}
k_{x\_x} &= k_{n2}n_x m_x \\
k_{x\_y} &= k_{n2}n_y m_x \\
k_{x\_z} &= k_{n2}n_z m_x \\
k_{x\_xy} &= 2k_{n1}n_x n_y m_x - \\
&\quad k_s n_x z_0 \\
k_{x\_xz} &= 2k_{n1}n_x n_z m_x + \\
&\quad k_s n_x y_0 \\
k_{x\_yz} &= 2k_{n1}n_y n_z m_x + \\
&\quad k_s n_y y_0 - k_s n_z z_0 \\
k_{x\_xx} &= k_{n1}n_x^2 m_x \\
k_{x\_yy} &= k_{n1}n_y^2 m_x - k_s n_y z_0 \\
k_{x\_zz} &= k_{n1}n_z^2 m_x + k_s n_z y_0
\end{aligned}
\qquad
\begin{aligned}
k_{y\_x} &= k_{n2}n_x m_y \\
k_{y\_y} &= k_{n2}n_y m_y \\
k_{y\_z} &= k_{n2}n_z m_y \\
k_{y\_xy} &= 2k_{n1}n_x n_y m_y + \\
&\quad k_s n_y z_0 \\
k_{y\_xz} &= 2k_{n1}n_x n_z m_y + k_s n_z z_0 - \\
&\quad k_s n_x x_0 \\
k_{y\_yz} &= 2k_{n1}n_y n_z m_y - \\
&\quad k_s n_y x_0 \\
k_{y\_xx} &= k_{n1}n_x^2 m_y + k_s n_x z_0 \\
k_{y\_yy} &= k_{n1}n_y^2 m_y \\
k_{y\_zz} &= k_{n1}n_z^2 m_y - k_s n_z x_0
\end{aligned}
\qquad
\begin{aligned}
k_{z\_x} &= k_{n2}n_x m_z \\
k_{z\_y} &= k_{n2}n_y m_z \\
k_{z\_z} &= k_{n2}n_z m_z \\
k_{z\_xy} &= 2k_{n1}n_x n_y m_z + k_s n_x x_0 - \\
&\quad k_s n_y y_0 \\
k_{z\_xz} &= 2k_{n1}n_x n_z m_z - k_s n_z y_0 \\
k_{z\_yz} &= 2k_{n1}n_y n_z m_z + k_s n_z x_0 \\
k_{z\_xx} &= k_{n1}n_x^2 m_z - k_s n_x y_0 \\
k_{z\_yy} &= k_{n1}n_y^2 m_z + k_s n_y x_0 \\
k_{z\_zz} &= k_{n1}n_z^2 m_z
\end{aligned}
\tag{6}
$$

$$
\begin{aligned}
k_s &= -A(1-C_s) \\
k_{n1} &= -2AC_s \\
k_{n2} &= -2AC_d\,/\,3
\end{aligned}
\qquad
\vec{M} = \begin{bmatrix} m_x \\ m_y \\ m_z \end{bmatrix} = \vec{r}_0 \times \vec{n} = \begin{bmatrix} y_0 n_z - z_0 n_y \\ z_0 n_x - x_0 n_z \\ x_0 n_y - y_0 n_x \end{bmatrix}
\tag{7}
$$

where $\vec{r}_0 = [x_0 \;\; y_0 \;\; z_0]^{\mathrm{T}}$ is the vector from the spacecraft center of mass to the center of pressure of the plate, $\hat{n}$ is the unit, outward-pointing vector normal to the plate, and A is the area of the plate.

For each plate, the vector $\vec{r}_p = \begin{bmatrix} x_p & y_p & z_p \end{bmatrix}^T$ from the origin to the plate center of pressure is constant in the shade frame so that $\vec{r}_0 = \vec{r}_p - \vec{r}_c$ where $\vec{r}_c$ is the location of the spacecraft center of mass.

The total solar torque from the collection of plates that make up the shade can be expressed as the sum of the individual contributions of each plate when the plates do not overlap and for Sun directions where there is no shadowing of one plate by any of the other plates. This is the case for all Sun directions in the keep-in zone for MESSENGER. The total solar torque is given by the summation below

$$\begin{aligned} N_j &= \sum_{i=1}^{p} N_j^i \qquad j \in \{x, y, z\} \\ &= P\left\{ \left(\sum_{i=1}^{p} k_{j\_x}^i \right) s_x + \left(\sum_{i=1}^{p} k_{j\_y}^i \right) s_y + \left(\sum_{i=1}^{p} k_{j\_z}^i \right) s_z + \left(\sum_{i=1}^{p} k_{j\_xy}^i \right) s_x s_y + \left(\sum_{i=1}^{p} k_{j\_xz}^i \right) s_x s_z + \left(\sum_{i=1}^{p} k_{j\_yz}^i \right) s_y s_z + \right. \\ &\qquad \left. \left(\sum_{i=1}^{p} k_{j\_xx}^i \right) s_x^2 + \left(\sum_{i=1}^{p} k_{j\_yy}^i \right) s_y^2 + \left(\sum_{i=1}^{p} k_{j\_zz}^i \right) s_z^2 \right\} \end{aligned} \tag{8}$$

where p is the total number of plates and there is a separate set of coefficients for each plate. In the most general case, all of the parameters $\vec{r}_0$, $\hat{n}$, A, C_s, and C_d can be different for each plate. It is often convenient to assume that C_s and C_d are the same for all plates in the shade, but this is not dictated by the formulation of the solar torque equations.

Solar Torque Model for the Solar Panels

The solar torque acting on the spacecraft from the two solar panels is derived in a manner similar to that for a flat plate. A panel frame is introduced whose origin is the same as the body frame origin and whose axes are ideally exactly aligned with the axes of the body frame. Each solar panel is assumed to rotate about the X-axis of the panel frame. The surface normal vector $\hat{n}$ in Eq. (1) is constant over the panel and is given by

$$\hat{n} = \begin{bmatrix} 0 & -\cos\phi & -\sin\phi \end{bmatrix}^{\mathrm{T}} \tag{9}$$

where ϕ is the rotation angle in the YZ plane measured positive about the +X-axis with the zero reference taken as the –Y-axis. Note that $\hat{n}$ points away from the side of each panel that is covered with solar cells. Performing the integration indicated in Eq. (2) gives

$$\vec{N} = \begin{bmatrix} N_x & N_y & N_z \end{bmatrix}^{\mathrm{T}} = -P\left\{ (1 - C_s) A (\hat{n} \cdot \hat{s}) \{ \vec{r}_0 \times \hat{s} \} + 2 [C_s (\hat{n} \cdot \hat{s}) + 1/3 C_d] A (\hat{n} \cdot \hat{s}) \{ \vec{r}_0 \times \hat{n} \} \right\} \tag{10}$$

where A is the total area of the panel, C_s and C_d are the specular and diffuse reflectivity coefficients for the side of the panel populated with solar cells, and $\vec{r}_0$ is the vector from the spacecraft center of mass to the center of pressure of the panel. Since the panel rotation axis (X) passes through the center of the panel,

$$\vec{r}_0 = \vec{r}_p - \vec{r}_c = \begin{bmatrix} x_p \\ 0 \\ 0 \end{bmatrix} - \begin{bmatrix} c_x \\ c_y \\ c_z \end{bmatrix} \tag{11}$$

where $\vec{r}_c$ is the location of the spacecraft center of mass and $\vec{r}_p$ is the location of the center of the panel in the panel frame.

System Momentum Model

The total system momentum of the spacecraft is the integral over time of all external torques acting on the spacecraft. The total external torque is the sum of the solar torques from the sunshade and the solar panels

$$\begin{aligned}\vec{T} &= \vec{T}_{sh} + \vec{T}_{pl} + \vec{T}_{pr} \\ &= Q_{sh}^{sc}\vec{N}_{sh} + Q_{sp}^{sc}\vec{N}_{pl} + Q_{sp}^{sc}\vec{N}_{pr}\end{aligned} \tag{12}$$

where $\vec{N}_{sh}$, $\vec{N}_{pl}$, and $\vec{N}_{pr}$ are the solar torques from the sunshade and the two solar panels in the shade or panel frame, Q_{sh}^{sc} and Q_{sp}^{sc} are the transformation matrices giving the orientation of the shade and panel frames relative to the body frame, $\vec{T}_{sh}$, $\vec{T}_{pl}$, and $\vec{T}_{pr}$ are the solar torques in the body frame. Recall that ideally the shade, panel, and body frames are co-aligned so that Q_{sh}^{sc} and Q_{sp}^{sc} are identity matrices. They are included in Eq. (12) to account for slight misalignments of the sunshade and panels relative to the spacecraft body frame; it is expected that these offsets will be small. Finally the total system momentum (expressed in the body frame) is given by

$$\vec{H} = \int \vec{T} dt \tag{13}$$

MOMENTUM ALTERATION USING SOLAR TORQUE

Although the solar torques are generally considered disturbances that must be compensated by the control system, they can also be used as a passive means of altering system momentum. By selectively choosing the spacecraft attitude, the resulting cumulative effect of solar torque can cause components of the system momentum vector to reach a desired target value over a specified time period. If other objectives and constraints on spacecraft attitude can still be met along with the placement of the Sun direction, changing system momentum can be accomplished concurrently with normally scheduled spacecraft activities. This strategy was used successfully for the Near Earth Asteroid Rendezvous mission and will be used for MESSENGER. This section first explains how the azimuth and elevation components of the Sun direction can be independently chosen to alter the Z and X components of system momentum. Next, the formulation for specifying spacecraft attitude to achieve the desired Sun direction while simultaneously maintaining high-gain antenna communication with Earth is presented.

Targeting Momentum Components by Choice of Sun Direction

Given their relative sizes and placement, the solar torque generated by the sunshade is much greater than that produced by the solar panels. If the spacecraft maintains a fixed attitude for some time period Δt, the change in system momentum over that period will be the product of the constant solar torque from the sunshade $\vec{N}_{sh}$ and the elapsed time Δt. If the change in momentum is specified, the problem then becomes one of solving for a Sun direction that produces the necessary value for $\vec{N}_{sh}$. It is not possible to simultaneously target all three components of the system momentum vector using solar torque since there are only two free variables – the azimuth and elevation angles of the Sun direction. But in the case of MESSENGER, it is possible to manipulate the momentum components in two of the three axes through independent choices of azimuth and elevation of the Sun direction.

For convenience in the following derivation, assume that Q_{sh}^{sc} is the identity matrix so that $\vec{N}_{sh} = \vec{T}_{sh}$. Let $\vec{H}_0$ be the system momentum at the start of the time window and suppose that the

desired momentum value at the end of the window is $\vec{H}_t$. Then $\vec{H}_t = \vec{H}_0 + \vec{T}_{sh}\Delta t$ or $\vec{T}_{sh} = (\vec{H}_t - \vec{H}_0)/\Delta t$ where $\vec{T}_{sh}$ is a function of the Sun direction $\hat{s}$. The Sun keep-in-zone for MESSENGER restricts A_s and E_s to ranges where the small angle approximations $\cos\theta \approx 1$ and $\sin\theta \approx \theta$ can be applied to express $\hat{s}$ as

$$\hat{s} = \begin{bmatrix} \cos\mathrm{E}_s \sin\mathrm{A}_s & -\cos\mathrm{E}_s \cos\mathrm{A}_s & -\sin\mathrm{E}_s \end{bmatrix}^{\mathrm{T}} \approx \begin{bmatrix} \mathrm{A}_s & -1 & -\mathrm{E}_s \end{bmatrix} \tag{14}$$

Substituting these expressions for $\hat{s}_x$, $\hat{s}_y$, and $\hat{s}_z$ into Eq. (3) for $\vec{T}_{sh}$ and keeping only the linear terms in A_s and E_s, the equation for $\vec{T}_{sh}$ becomes

$$\vec{T}_{sh} = \begin{bmatrix} (k_{x\_x} - k_{x\_xy})\mathrm{A}_s + (k_{x\_yz} - k_{x\_z})\mathrm{E}_s + (k_{x\_yy} - k_{x\_y}) \\ (k_{y\_x} - k_{y\_xy})\mathrm{A}_s + (k_{y\_yz} - k_{y\_z})\mathrm{E}_s + (k_{y\_yy} - k_{y\_y}) \\ (k_{z\_x} - k_{z\_xy})\mathrm{A}_s + (k_{z\_yz} - k_{z\_z})\mathrm{E}_s + (k_{z\_yy} - k_{z\_y}) \end{bmatrix} \tag{15}$$

For the cylindrical shade, the coefficients k_{x_x}, k_{x_xy}, k_{y_y}, k_{y_z}, k_{y_yy}, k_{z_z}, and k_{z_yz}, are zero. The set of rectangular plates for the sunshade retains the lateral symmetry of the cylinder. For each plate, $n_z = 0$ so that the sums in Eq. (8) for k_{y_z}, k_{z_z}, and k_{z_yz} are zero for the plate model also. Further, the n_x components either occur in pairs of opposite sign or are zero, causing the terms for k_{x_x}, k_{x_xy}, k_{y_y}, and k_{y_yy} in Eq. (8) to sum to zero over the entire shade. This means that the expression for $\vec{T}_{sh}$ can be further simplified to

$$\vec{T}_{sh} = \begin{bmatrix} (k_{x\_yz} - k_{x\_z})\mathrm{E}_s + (k_{x\_yy} - k_{x\_y}) \\ (k_{y\_x} - k_{y\_xy})\mathrm{A}_s + (k_{y\_yz})\mathrm{E}_s \\ (k_{z\_x} - k_{z\_xy})\mathrm{A}_s + (k_{z\_yy} - k_{z\_y}) \end{bmatrix} \tag{16}$$

Note that the X component of $\vec{T}_{sh}$ is now only a function of E_s while the Z component is a function only of A_s. The X and Z components of system momentum can be changed to some specified value over the time window Δt by choosing the Sun azimuth and elevation angles to be

$$\begin{aligned} \mathrm{E}_s &= \left\{(T_{sh})_x - (k_{x\_yy} - k_{x\_y})\right\} / (k_{x\_yz} - k_{x\_z}) & (\vec{T}_{sh})_x &= \left\{(\vec{H}_t)_x - (\vec{H}_0)_x\right\} / \Delta t \\ \mathrm{A}_s &= \left\{(T_{sh})_z - (k_{z\_yy} - k_{z\_y})\right\} / (k_{z\_x} - k_{z\_xy}) & (\vec{T}_{sh})_z &= \left\{(\vec{H}_t)_z - (\vec{H}_0)_z\right\} / \Delta t \end{aligned} \tag{17}$$

This can easily be generalized for cases where $Q_{sh}^{sc} \neq \mathrm{I}$ by first transforming the target momentum vector to the shade frame, determining the required direction for the Sun in that frame, and then transforming back to the body frame to derive the necessary spacecraft attitude.

As expected, the full momentum vector cannot be manipulated. The Y component of the solar torque is a function of both A_s and E_s, and its value will be fixed by the choices made to alter the X and Z components of system momentum. Fortunately, this torque is generally an order of magnitude less than the X and Z components, and simulations have shown that momentum does not accumulate as rapidly on this axis as on the X- or Z-axes.

Spacecraft Attitude for Simultaneous Downlink and Solar Torque Momentum Change

MESSENGER will complete two orbits about the planet every 24 hours during the full year of

Mercury observations after orbit insertion. The current operational plan calls for the spacecraft to perform science observations for 16 of every 24 hours, or 1 and 1/3 orbits. The remaining 8 hours or 2/3 orbit will be used to downlink science and spacecraft engineering data to Earth. During the science observation portion of the day, the spacecraft attitude is completely determined by the dual goals of pointing the boresight of one or more of the science instruments at some target on or near the planet and keeping the direction to the Sun as close as possible to the –Y axis so that the sunshade adequately shields the spacecraft from sunlight. Momentum will accumulate due to solar torque as pitch rotations are made to obtain the requisite viewing geometry for the instruments. This leaves only the downlink period available for momentum management either through thruster dumps or through offsets of the nominal attitude to take advantage of solar torque. Fortunately, the high-gain antenna design and placement does allow spacecraft attitude offsets to put the Sun direction in a location where solar torque will target a desired momentum state. The algorithm for computing the spacecraft attitude that simultaneously puts the Sun in a desired direction in the body frame and the direction to Earth in the field-of-view of one of the high-gain antennas is described below.

In the absence of any momentum targeting, the default downlink attitude while in Mercury orbit is to have the spacecraft –Y-axis pointing along the direction to the Sun and the direction to Earth lying in one of the quadrants of the XY plane covered by one of the phased-array antennas. The choice of which quadrant, and hence, which antenna to use is dictated by the separation angle between the vectors to the Earth and the Sun as seen from the spacecraft, denoted θ_{es}. When $\theta_{es} < \pi/2$, the Earth vector must lie in the -X, -Y quadrant so that the antenna mounted on the sunshade is used. When $\theta_{es} > \pi/2$, the Earth vector must lie in the +X,+Y quadrant, and the antenna mounted on the back side of the spacecraft structure is used. In other words, the unit vector to Earth must have $E_e = 0$ and $-\pi/2 < \mathrm{A}_e < 0$ or $\pi/2 < \mathrm{A}_e < \pi$. The transformation Q_{J2}^{D} from the inertial frame to the body frame for this default attitude can be expressed as

$$Q_{J2}^{D} = \begin{bmatrix} \hat{i}_x{}^T \\ \hat{i}_y{}^T \\ \hat{i}_z{}^T \end{bmatrix} \quad \begin{array}{l} \hat{i}_y = -\hat{i}_s \\ \hat{i}_z = \left(\hat{i}_e \times \hat{i}_s\right) \Big/ \left\| \left(\hat{i}_e \times \hat{i}_s\right) \right\| \quad \textit{for } \theta_{es} < \pi/2 \quad \textit{or} \quad \left(\hat{i}_s \times \hat{i}_e\right) \Big/ \left\| \left(\hat{i}_s \times \hat{i}_e\right) \right\| \quad \textit{for } \theta_{es} > \pi/2 \\ \hat{i}_x = \left(\hat{i}_y \times \hat{i}_z\right) \Big/ \left\| \left(\hat{i}_y \times \hat{i}_z\right) \right\| \end{array} \tag{18}$$

where $\hat{i}_e$ and $\hat{i}_s$ are unit vectors from spacecraft to Sun and Earth in the EME2000 inertial reference frame, known from planetary ephemerides and navigation solutions for the spacecraft trajectory.

To find the attitude offset from this default attitude that satisfies the solar torque target and maintains the Earth direction in a quadrant of the XY plane for downlink, first perform a rotation that puts the Sun direction at the desired location for solar torque. Let the desired Sun direction be represented by $\hat{s}$ as given in Eq. (14) where A_s and E_s are computed from Eq. (17). This rotation Q_D^1 is expressed by the X-Z Euler rotation sequence

$$Q_D^1 = Q_z(-\mathrm{A}_s)\, Q_x(-\mathrm{E}_s) \tag{19}$$

where Q_z is a rotation about the Z-axis by the azimuth angle and Q_x is a rotation about the X-axis by the elevation angle. The direction to Earth in this intermediate frame is given by $\hat{e}_1 = Q_D^1 Q_{J2}^D \hat{i}_e$.

Next perform a rotation about the Sun line from this intermediate attitude such that the Earth line moves back into the XY plane. Since the Sun direction is constant under this final rotation, the possible final locations for the Earth vector can be found using the spherical triangle shown in Figure 3. From the law of cosines,

$$\cos\delta = \cos\theta_{es} / \cos \mathrm{E}_s \tag{20}$$

After this final rotation, the unit vector to Earth in the body frame will be $\hat{e}_2 = \begin{bmatrix} \sin(\mathrm{A}_s \pm \delta) & -\cos(\mathrm{A}_s \pm \delta) & 0 \end{bmatrix}^{\mathrm{T}}$.

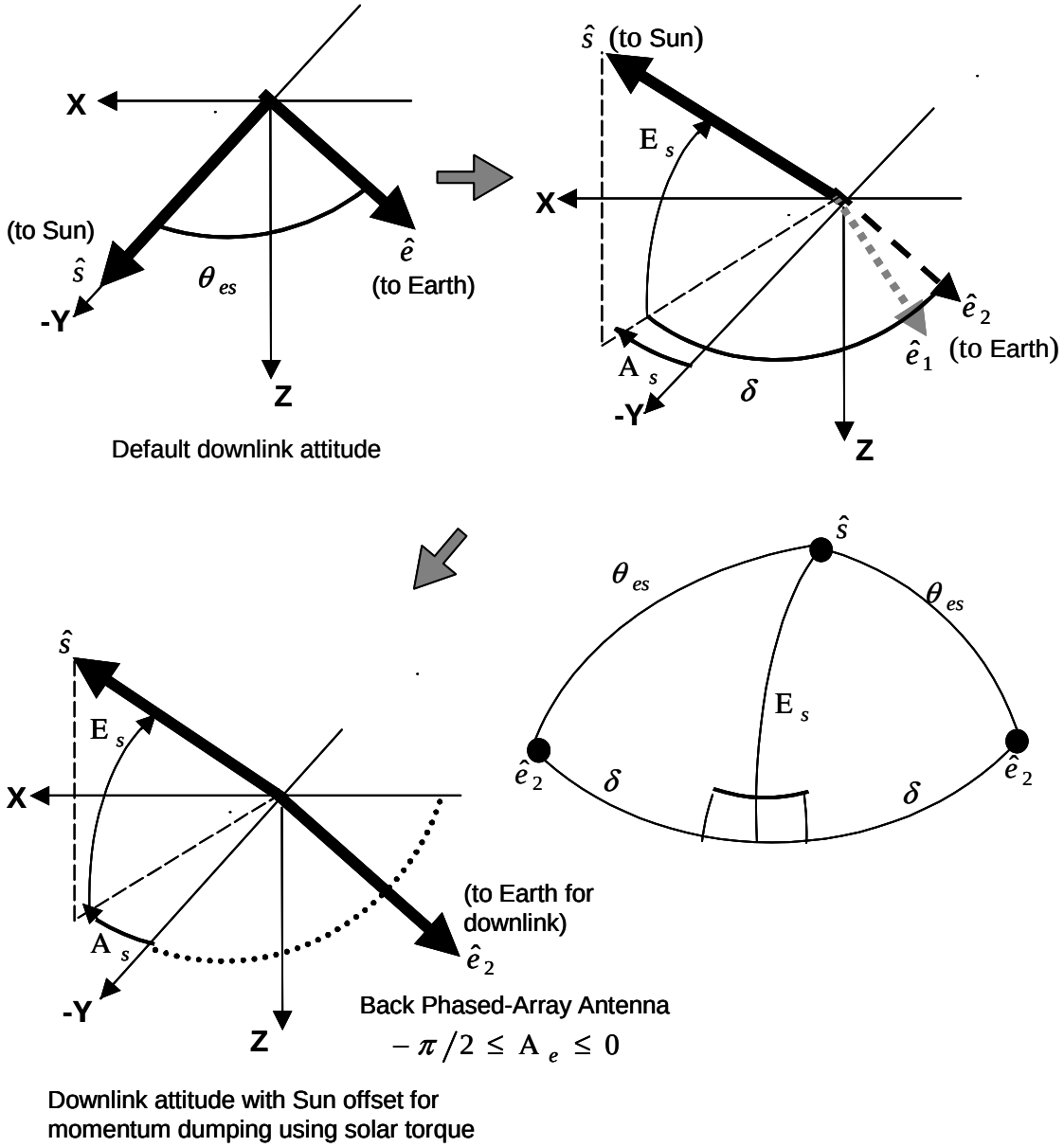

Figure 3 Rotations to Put the Sun in a Desired Direction while Keeping the Earth line in the XY Plane

The rotation angle about the Sun line is the angle between the plane containing the vectors to the Sun and the Earth in the intermediate frame and the plane containing the vectors to the Sun and the Earth in the XY plane, $\hat{e}_2$. This angle, denoted β, is found using the normals to these two planes as shown below

$$\beta = \cos^{-1}(\hat{\eta}_1 \cdot \hat{\eta}_2) \quad \text{where} \quad \hat{\eta}_1 = (\hat{s} \times \hat{e}_1) / \left\| \hat{s} \times \hat{e}_1 \right\| \quad \textit{and} \quad \hat{\eta}_2 = (\hat{s} \times \hat{e}_2) / \left\| \hat{s} \times \hat{e}_2 \right\| \tag{21}$$

The sign of β depends on which side of the $\hat{s}, \hat{e}_2$ plane contains the $\hat{e}_1$ vector:

$$\beta > 0 \quad if \quad \eta_2 \cdot \hat{e}_1 > 0 \qquad \text{or} \qquad \beta < 0 \quad if \quad \eta_2 \cdot \hat{e}_1 < 0$$

Let Q_1^2 be the rotation matrix representing the rotation about $\hat{s}$ by angle β; then the rotation from the inertial frame to the desired offset downlink attitude is

$$Q_{J2}^2 = Q_1^2 \; Q_D^1 \; Q_{J2}^D \tag{22}$$

The spacecraft attitude constraints and the inherent geometric constraints place limits on the ranges for Sun and Earth azimuth and elevation angles. Depending on the starting and desired ending momentum values, Eq. (17) can produce values of A_s and E_s that are outside the Sun keep-in zone. A_s and E_s are then set such that the Sun direction lies on the boundary of the keep-in-zone as close as possible to the direction desired for momentum targeting. The Earth-Sun geometry places another restriction on E_s. Solutions to Eq. (20) for δ only exist when $\mathrm{E}_s \le \theta_{es}$. This supercedes the Sun keep-in zone limitation in cases where θ_{es} is smaller than the keep-in zone elevation boundary in magnitude. Finally, A_e must fall in one of the phased-array antenna quadrants. In general, there are two solutions for δ and hence β; the choice of which to use is made based on the resulting value of A_e. In rare cases, neither choice will satisfy the quadrant restrictions on A_e and it is necessary to adjust A_s and E_s until A_e moves back into one of the phased-array antenna quadrants. All these constraints mean that the target value for system momentum components may not be met by the end of the downlink period, but the solar torque will act to move the momentum components as close as possible to the target values while still satisfying the constraints on A_s, E_s, and A_e.

MOMENTUM MANAGEMENT STRATEGIES

One of MESSENGER's science goals is to characterize the structure of Mercury's core.[1] Insight into this internal structure can be achieved by attempting to determine the libration amplitude and gravitational field structure of Mercury through a combination of radio science and laser altimetry. An accurate characterization is dependent on minimizing perturbations to the spacecraft's trajectory from sources other than the planet's gravitational field. One of the major sources of non-gravitational forces acting on the trajectory are velocity changes induced whenever thrusters are used. Since thrusters must occasionally be used to unload momentum stored in the reaction wheels, it is highly desirable to manage system momentum so that thruster dumps are needed as infrequently as possible. Current mission requirements state that momentum dumps using thrusters must be separated by a period of at least five days during the orbital phase of the mission.

The momentum storage capacity of the reaction wheels is one obvious factor that can be used to reduce the frequency of thruster dumps. Larger wheels can store more momentum before requiring it to be unloaded using thrusters. Unfortunately, larger wheels have more mass and consume more power, both of which are at a premium for the MESSENGER spacecraft. Standard commercially available wheels can be machined to have a storage capacity between 4 and 12 Nms per wheel with a total mass between 12 and 20 kg for four wheels. Determining an appropriate size for the wheels has been one of the primary motivations for developing the momentum models and simulating momentum accumulation during orbital operations. The current mass allocation for the reaction wheels is 17 kg which will allow 8 Nms momentum storage per wheel. This allocation is a compromise between guidance and control desires and overall spacecraft mass and power resources based on the results of orbital simulations presented below.

Another strategy that can reduce the need for thruster dumps is to use the solar torque acting

on the sunshade during the 8-hour downlink periods as discussed in the previous section. One issue that arises with this strategy is the choice of the target values for the X and Z momentum components at the end of the downlink period. The simplest approach is to set the target value to zero to remove all momentum accumulated in these axes prior to that downlink period. This procedure is called “reactive” solar torque dumping since it only responds to the momentum value at the current time. A more complex approach that may prove more useful over the long term is to select non-zero target values that will maximize the time required to build up to a point where a thruster dump is required after the downlink period. Ideally, it might even be possible to keep the momentum within a deadband where no thruster dumps are needed by selecting a profile of target values for several consecutive downlink periods that bias the system momentum to offset anticipated momentum accumulation during the intervening science observation periods. This approach is called “predictive” solar torque dumping since it obviously requires knowledge of future spacecraft attitude history so that momentum changes can be anticipated. With such a strategy the effectiveness of the passive dumps can be maximized, but it does complicate ground operations and place constraints on the process of planning and coordinating future spacecraft attitude changes for science and engineering activities.

Realistically, the constraints on the downlink attitude will limit the values to which momentum can be targeted with solar torque, and thruster dumps will eventually still be needed. Similar issues arise in making the choice of the momentum target to be achieved with a thruster dump. One choice is to target to a zero momentum vector to remove all accumulated momentum. A more sophisticated choice is to target to a biased vector that will increase the time before one or more of the momentum components will again reach the limit where a dump is required. As was the case for the solar torque target, this methodology requires some ability to predict the future momentum accumulation after the dump. For example, if it is known that the X component of momentum will move in the negative direction after the dump, the target value could be chosen to be at the positive magnitude limit. The X momentum would then have to decrease from the positive limit through zero to the negative limit, which would take more time than decreasing from zero to the negative limit.

SIMULATION OF ON-ORBIT MOMENTUM ACCUMULATION

The extent to which any or all of the momentum management strategies are needed and their effectiveness depend on the actual momentum accumulation experienced by the spacecraft in orbit about Mercury. This, in turn, depends on spacecraft attitude history and assumptions for parameters in Eqs. (3) and (10) for solar torque from the sunshade and solar panels. In order to compare the different strategies and the relative influence of geometric and material properties that determine solar torque, a simulation has been developed that can compute momentum over time, apply thruster dumps, and use sunshade solar torque to passively alter system momentum during the downlink periods.

Spacecraft attitude during the 16-hour science observation periods is computed using a preliminary set of rules developed by MESSENGER project team members.[6] These rules rotate away from the default attitude about the X axis, placing the Z axis in a direction that optimizes viewing conditions for one or more of the instruments based on the spacecraft’s location relative to the Sun and Mercury. The resulting attitudes are constrained such that Sun elevation angle stays within the keep-in zone limits. Spacecraft attitude during the 8-hour downlink periods is either set to the default attitude or offset based on momentum targeting using sunshade solar torque. If reactive momentum targeting is used, the Sun direction is computed to achieve pre-specified values of momentum components in either X or Z or both, subject to Sun keep-in zone and Earth-antenna viewing constraints. Alternately, the predictive targeting strategy can be selected where the momentum targets are internally computed to follow a profile that attempts to minimize future momentum accumulation. The relative positions and velocities of MESSENGER, the Sun, Earth, and Mercury are taken from trajectory solutions described in (Ref. 7).

Thruster dumps are inserted whenever one or more components of the momentum vector exceed a pre-specified magnitude limit. Thruster dumps are modeled as instantaneous changes in the value of the system momentum vector. Momentum vector components whose magnitude exceeds the dump threshold are re-initialized to a value having another pre-specified magnitude and opposite in sign from the value at the time the dump is triggered. Momentum magnitude values after the dump are most often set to the same value as the dump threshold, but cases using zero post-dump magnitudes have also been considered. Thruster dumps can be effectively eliminated from the simulation by setting the dump magnitude threshold to a very large number. The momentum magnitude limit that triggers a thruster dump is selected to reflect the total momentum storage capacity of the four reaction wheels for a given alignment of their rotation axes relative to the body frame.

System momentum is computed as the integral of solar torques due to the sunshade or to both the sunshade and the solar panels. The simulation accepts a value for solar flux that determines the value of P used in Eqs. (4) and (6). This is usually set to a value commensurate with Mercury's mean distance from the Sun. The simulation also accepts specifications for sunshade and solar panel, shape, size, and material reflectance properties. If a cylinder model is selected for the shade, values can be given for R, h_0, θ_0, C_s, C_d, and $\vec{r}_c$. For a set of plates, values for $\vec{r}_0$, $\hat{n}$, A, C_s, and C_d can be entered for each plate. The initialization procedure computes values for the k coefficients in Eq. (3) which are held constant over the simulation time period. Similarly for each plate that represents a solar panel, values for $\vec{r}_c$, $\vec{r}_p$, $\hat{n}$, A, C_s, and C_d can be given. A value for Q_{sh}^{sc} or Q_{sp}^{sc} can also be specified, although almost all cases to date have used $Q_{sh}^{sc} = Q_{sp}^{sc} = \mathrm{I}$. The orientation of the panels can either be set to a fixed angle in the spacecraft body frame or set to maintain a fixed angle relative to the Sun direction. In the latter case, the simulation computes the orientation relative to the spacecraft body frame needed to maintain the Sun-relative angle as the spacecraft attitude changes.

Simulation Results

The spacecraft attitude profile for science observations repeats roughly every 88 days, reflecting Mercury's orbital period. A representative 90-day period out of the full Earth year that MESSENGER will remain in orbit was chosen to analyze momentum accumulation and management strategies. Initial simulations used a cylindrical shade and focused only on the momentum accumulation without invoking any momentum management strategies. These cases studied the momentum distribution and rate of accumulation in each of the body axes as the sunshade geometry and reflectance properties were varied. The most significant factor influencing the momentum accumulation was found to be the offset between the spacecraft center of mass and the "center" of the shade, represented by $\vec{r}_c$. The largest amount of momentum accumulated in the X direction; accumulation in the Z direction was somewhat less, while accumulation in the Y direction was an order of magnitude smaller than either the X or Z values. Variation of specular and diffuse reflectivity coefficients did slightly change the momentum accumulation, but to a much lesser extent than the center of mass offsets.

Given the spacecraft's mechanical configuration and predictions of fuel mass motion during the orbital phase, offsets between the shade origin and the center of mass are expected to be larger along the Z axis. The next round of momentum simulations compared three different dumping strategies for center of mass offsets of 0, 2.5, or 5 cm in the Z direction, with no offset in the X or Y directions. The assumptions for shade shape and size are shown in Table 1. Thruster dumps were inserted in all cases using one of two momentum magnitude thresholds. A threshold of 4 Nms was used to represent small wheels with 4 Nms momentum storage capacity, while the threshold was increased to 7 Nms to represent large wheels with 12 Nms storage capacity. The other two momentum management strategies combined passive dumping with thruster dumps.

The passive solar torque dumping was applied in either the reactive or predictive sense.

Table 1

SUNSHADE AND SOLAR PANEL CHARACTERISTICS FOR SIMULATIONS

P - Solar pressure at $D_s = 0.3$ AU		5.0145e-05 N/m^2	
Sunshade			
Alignment		$Q_{sh}^{sc} = \mathrm{I}$	
Cylindrical Section			
$\vec{r}_c{}^T$ - center of mass location relative		[0 0 0] m	
R - Radius		0.991 m	
$2h_0$ - Total height		2.489 m	
$2\theta_0$ - Total angle subtended		122°	
C_s - Specular reflectivity coefficient		0.15	
C_d - Diffuse reflectivity coefficient		0.35	
Contiguous Rectangular Plates			
Plate #	A -Area (m^2)	$\vec{r}_0{}^{\mathrm{T}} = \vec{r}_p{}^{\mathrm{T}}$ - Center Location (m)	$\hat{n}^{\mathrm{T}}$ - Normal Vector
1	1.169	[0.7442 –0.6657 0.0307]	[0.7071 –0.7071 0]
2	1.169	[-0.7442 –0.6657 0.0307]	[-0.7071 –0.7071 0]
3	0.8672	[0.39782 –0.9142 0.0307]	[0.3973 –0.9205 0]
4	0.8672	[-0.3978 -.09142 0.0307]	[-0.3907 –0.9205 0]
5	1.068	[0 –0.9864 0.0307]	[0 –1 0]
6	0.02052	[-0.2897 –0.9601 –1.218]	[-0.3907 –0.9205 0]
7	0.02052	[0.2897 –0.9601 –1.218]	[0.3907 –0.9205 0]
8	0.06409	[0 –0.9864 –1.218]	[0 –1 0]
C_s - Plate specular reflectivity coefficients		0.15	
C_d - Plate diffuse reflectivity coefficients		0.35	
Solar Panels			
Alignment		$Q_{sp}^{sc} = \mathrm{I}$	
Panel #		A - Area (m^2)	$\vec{r}_p{}^T$ - Center Location (m)
1		2.5	[2.28 0 0]
2		2.5	[-2.28 0 0]
C_s - Panel specular reflectivity coefficient			0.52
C_d - Panel diffuse reflectivity coefficient			0.07

Figures 4 and 5 show the time history of the X component of system momentum for the three different momentum management strategies with the thruster dump threshold set to the value for small wheels. The three plots in each figure show the X momentum accumulations when the Z component of the offset between the shade center and the spacecraft center of mass was set equal to 0, 2.5, or 5 cm, respectively. Figure 4 shows the cases where only thruster dumps were applied to reduce X-axis momentum. As expected, the dumps are inserted more frequently as the rate of momentum accumulation increases due to larger center of mass offsets. Figure 5 shows the benefits of adding passive dumping using solar torque during the downlink periods. The frequency of thruster dumps is reduced when solar torque dumping is employed in either the

reactive or predictive sense.

A different comparison between these cases is presented in Tables 2 and 3. Table 2 shows the total number of thruster dumps needed in the 90-day period for each of the three momentum management strategies for each value of the center of mass offset and thruster dump threshold. Table 3 shows the time separation of these thruster dumps. These statistics are important for detecting the combination of conditions that lead to violations of the mission requirement of at least five days separating consecutive thruster dumps. Not surprisingly, thruster dumps are required less frequently when center of mass offsets are small and wheel storage capacity is large. Violations of the 5-day separation requirement are observed in the more extreme cases with large Z components for the center of mass offset and small wheel storage capacity.

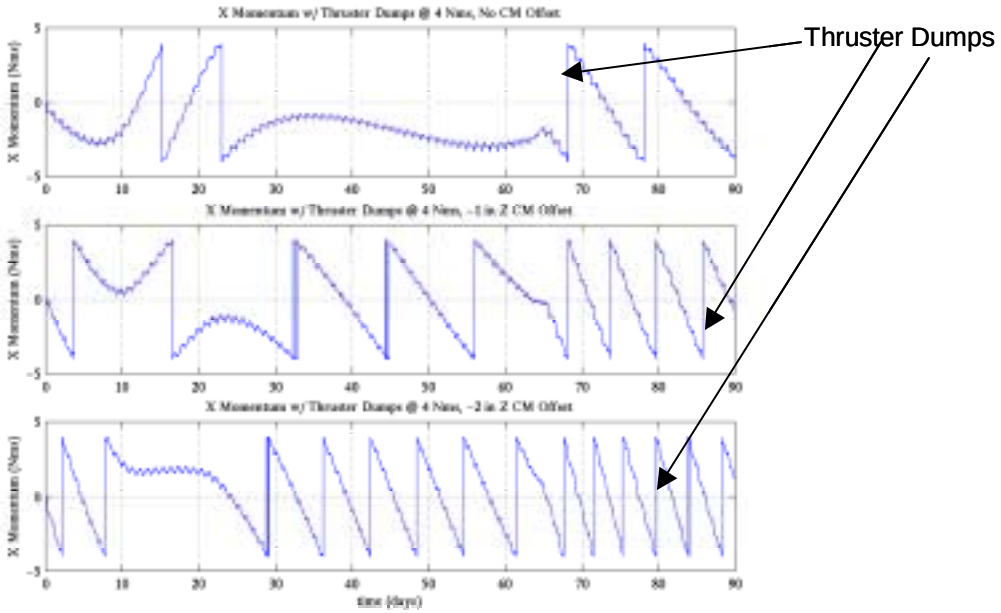

Figure 4 X-Axis Momentum Accumulation using Only Thruster Dumps for Cylindrical Sunshade

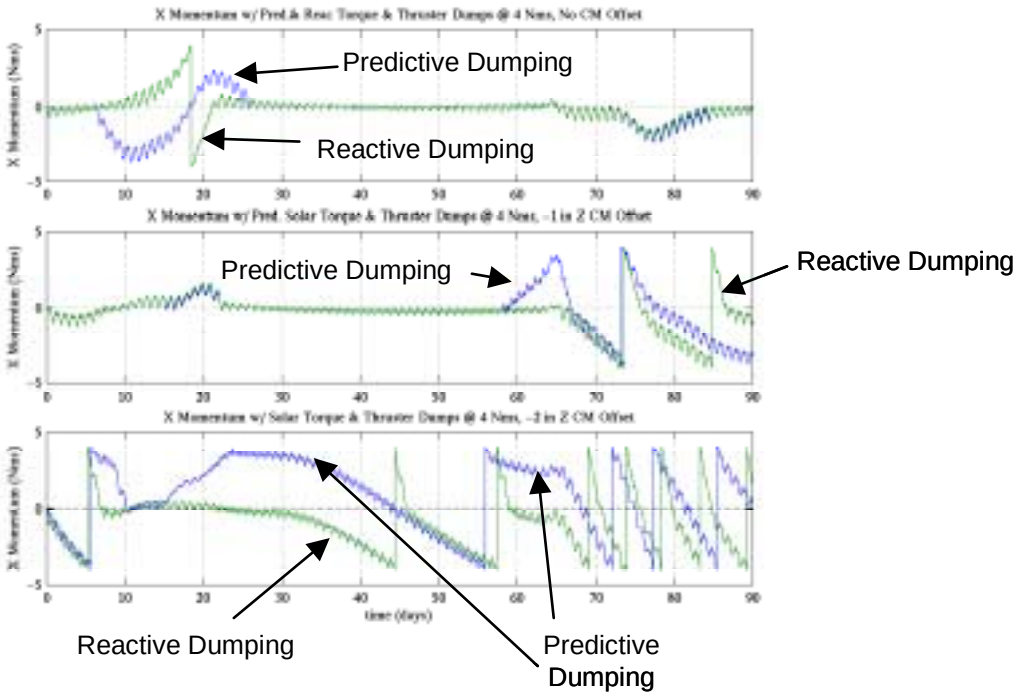

Figure 5 X-Axis Momentum Accumulation using Thruster Dumps and Reactive and Predictive Solar Torque Dumping for Cylindrical Sunshade

Table 2

NUMBER OF THRUSTER DUMPS FOR CYLINDRICAL SUNSHADE

Momentum Management Strategy	Z CM Offset		
	0 cm	-2.54 cm	-5.08 cm
Small Wheels (4 Nms thruster dump threshold)			
Thruster dumps only	4	9	14
Thruster dumps + reactive solar torque dumping	1	2	8
Thruster dumps + predictive solar torque dumping	0	1	5
Large Wheels (7 Nms thruster dump threshold)			
Thruster dumps only	2	6	8
Thruster dumps + reactive solar torque dumping	0	1	4
Thruster dumps + predictive solar torque dumping	0	0	2

Table 3

TIME SPACING OF THRUSTER DUMPS FOR CYLINDRICAL SUNSHADE

Momentum Management Strategy	Z CM Offset		
	0 cm	-2.54 cm	-5.08 cm
Small Wheels (4 Nms thruster dump threshold)			
Thruster dumps only	Closest 7 days Farthest 45 days Typical 7-10 days	Closest 5 days Farthest 15.5 days Typical 5-11 days	Closest 4 days Farthest 21 days Typical 4-6 days
Thruster dumps + reactive solar torque dumping	1 in 90 days	2, 11 days apart	Closest 4.5 days Farthest 39 days Typical 4-11 days
Thruster dumps + predictive solar torque dumping	N/A	1 in 90 days	Closest 5 days Farthest 50 days
Large Wheels (7 Nms thruster dump threshold)			
Thruster dumps only	2, 55 days apart	Closest 3.5 days Farthest 25.5 days Typical 10-20 days	Closest 7 days Farthest 25 days Typical 7-12 days
Thruster dumps + reactive solar torque dumping	N/A	1 in 90 days	Closest 7 days Farthest 53 days Typical 10-17 days
Thruster dumps + predictive solar torque dumping	N/A	N/A	2 , 11 days apart

The next series of simulations incorporated several changes intended to more realistically represent actual orbital conditions. First, solar torque from the solar panels was added as an additional source of momentum accumulation. The characteristics assumed for the solar panels are shown in Table 1. The panels' orientation was set to maintain an angle of 65° relative to the Sun direction. Second, the sunshade model was changed to a series of 8 rectangular plates with areas, normal vectors, and centers shown in Table 1. Finally, the momentum magnitude threshold that triggered thruster dumps was set to an intermediate value of 5.5 Nms, representing wheels with an intermediate storage capacity of 8 Nms. The shade shape and size and wheel storage capacity reflected MESSENGER's expected mechanical configuration and the available mass for reaction wheels at the time the simulations were performed.

The results obtained for these cases were not radically different than those obtained for the cases using a cylindrical shade. Momentum accumulation curves were very similar to those shown in Figures 4 and 5. The additional solar torque from the panels did not appreciably change the observed momentum accumulations. The dominant factor determining the frequency of thruster dumps continued to be offsets in the center of mass location. The cases using 0, 2.5, and 5 cm offsets in Z, with no offsets in X or Y were repeated. The number and spacing of thruster dumps was comparable to the cases using the cylindrical shade as shown in Tables 2 and 3. Additional cases were run using offsets in all 3 axes in order to test combined management of X and Z components of momentum. In these cases, the solar torque momentum targeting commanded non-zero elevation and azimuth angles for the Sun direction. Statistics on the occurrence of thruster dumps for these cases are also shown in Tables 4 and 5. As for the cases with a cylindrical shade, more frequent thruster dumps leading to violations of the 5-day separation were observed as the center of mass offset increased.

Table 4

NUMBER OF THRUSTER DUMPS FOR SUNSHADE OF RECTANGULAR PLATES

Intermediate Wheels (5.5 Nms thruster dump threshold)		
Momentum Management Strategy	Z CM Offset	
	-2.54 cm	-5.08 cm
Thruster dumps + reactive solar torque dumping	2	9
	Other CM Offsets (X, Y, Z)	
	0, 0, +2.54 cm	0, 0, +5.08 cm
Thruster dumps + reactive solar torque dumping	2	8
	+2.54, +2.54, +2.54 cm	-2.54, -2.54, -2.54 cm
Thruster dumps +reactive solar torque dumping	5	5

Table 5

TIME SPACING OF THRUSTER DUMPS FOR SUNSHADE OF RECTANGULAR PLATES

Intermediate Wheels (5.5 Nms thruster dump threshold)		
Momentum Management Strategy	Z CM Offset	
	-2.54 cm	-5.08 cm
Thruster dumps + reactive solar torque dumping	2, 11 days apart	Closest 4 days Farthest 30 days Typical 4-9 days
	Other CM Offsets (X, Y, Z)	
	0, 0, +2.54 cm	0, 0, +5.08 cm
Thruster dumps + reactive solar torque dumping	2, 4.5 days apart	Closest 3 days Farthest 12 days Typical 4-11 days
	+2.54, +2.54, +2.54 cm	-2.54, -2.54, -2.54 cm
Thruster dumps +reactive solar torque dumping	Closest 9 days Farthest 20 days	Closest 5 days Farthest 38 days

CONCLUSIONS

Managing system momentum is an ongoing challenge for the MESSENGER mission. The desire to minimize trajectory perturbations imposes restrictions on the use of thruster dumps to unload momentum from the reaction wheels once the spacecraft is in orbit about Mercury. Overall spacecraft mass constraints preclude carrying wheels with a large enough storage capacity to guarantee the desired 5-day spacing between thruster dumps. The analyses described in this paper have shown that it is possible to meet the requirement by augmenting thruster dumps with the selection of spacecraft attitudes where solar torque acts to alter system momentum. This strategy is most effective in cases where the offset between spacecraft center of mass and the “center” for solar torque generated by the sunshade is minimized. The spacecraft is being designed and will be fabricated to meet restrictions imposed on the center of mass location for momentum management purposes in addition to those imposed by launch vehicle and other engineering considerations.

The reliance on passive dumping using solar torque highlights the need for accurate and reliable models of momentum accumulation. The simulation tool presented in this paper represents an initial modeling effort that will be improved as part of advanced mission development. The solar pressure models will be extended to provide reasonable approximations for the torques acting at all spacecraft attitudes. This will allow simulations to be run for different parts of the cruise phase in addition to the orbital phase simulations performed to date. Provisions will also be added for the effects of shadowing at different attitudes and to accommodate periodic eclipses of the Sun during the orbital phase. The solar torque models will eventually be incorporated into an overall spacecraft dynamic simulation that includes other disturbance torques as well as flexible body effects.

Concurrently with improving the basic models, the simulation will be used to investigate many new operational scenarios. A refined set of science pointing rules is being developed that will have greater variation in the orbital pointing than those used here. Similar runs will be made with these new pointing profiles and using realistic transitions between different pointings to verify that there are no significant increases in the momentum accumulations observed thus far. Sensitivity to other model parameters such as non-uniform reflectivity coefficients will be explored. For example, cases will be run with the rectangular faces of the sunshade having different specular and diffuse coefficients. The effects of asymmetry will be explored through introduction of small misalignments between the body frame, the shade frame, and the panel frames and small offsets between orientations of the two solar panels. These cases will assist in validating and refining the basic strategies for momentum management outlined in this paper.

ACKNOWLEDGMENT

The work described in this paper was performed at The Johns Hopkins University Applied Physics Laboratory, under contract (NAS5-97271) with the National Aeronautics and Space Administration, Discovery Program Office.

REFERENCES

1. S. C. Solomon, et. al., “The MESSENGER Mission to Mercury: Scientific Objectives and Implementation,” *Planetary and Space Science*, in press 2001.

2. R. E. Gold, et. al., “The MESSENGER Mission to Mercury: Scientific Payload,” *Planetary and Space Science*, in press 2001.

3. A. G. Santo, et. al., “The MESSENGER Mission to Mercury: Spacecraft and Mission Design,” *Planetary and Space Science*, in press 2001.

4. V. L. Pisacane and R. C. Moore (eds), *Fundamentals of Space Systems*, Oxford Press, New York, 1994, pp 301-302.

5. H. S. Shapiro, “An Analytic Solution of Solar Radiation Torque Acting on a Cylindrical Surface,” (internal document), JHU/APL IOM SRM-00-067, August 9, 2000.

6. T. H. Choo, S. L. Murchie, and J. S. Jen, “The MESSENGER Science Planning Tool,” submitted for presentation at the Mercury: Space Environment, Surface and Interior Workshop, Chicago, IL, October 4-5, 2001.

7. J. V. McAdams, R. W. Farquhar, and C. L. Yen, “Improvements in Trajectory Optimization for MESSENGER: The First Mercury Orbiter Mission,” Paper AAS-01-458, AAS/AIAA Astrodynamics Specialist Conference, Quebec City, Quebec, Canada, July 30-August 2, 2001.